American Journal of Climate Change, 2016, 5, 77-87
Published Online March 2016 in SciRes. http://www.scirp.org/journal/ajcc
http://dx.doi.org/10.4236/ajcc.2016.51009

Spatial Distribution of CO_2 Concentration over South America during ENSO Episodes by Using GOSAT Data

Zhongyi Sun[1*], Xiufeng Wang[2], Hiroshi Tani[2], Guosheng Zhong[1], Shuai Yin[1]

[1]Graduate School of Agriculture, Hokkaido University, Sapporo, Japan
[2]Research Faculty of Agriculture, Hokkaido University, Sapporo, Japan
Email: *sunzy025@env.agr.hokudai.ac.jp

Received 23 February 2016; accepted 28 March 2016; published 31 March 2016

Abstract

Carbon dioxide (CO_2) is one of the most important greenhouse gases; its concentration and distribution have important implications on climate change. The El Niño Southern Oscillation (ENSO) is the Earth's strongest climate fluctuation on inter-annual time scales and has global impacts. However, to date, there is no research on how ENSO affects the spatial distribution of CO_2 concentration. In this study, we used spatial CO_2 data from the ENVIronmentSATellite (ENVISAT) and the Greenhouse Gases Observing Satellite (GOSAT), the long duration monthly mean atmospheric CO_2 from Mauna Loa Observatory, Multivariate ENSO Index (MEI) from Earth System Research Laboratory to analyze the way that ENSO affects spatial distribution of CO_2 concentration in South America, which is affected by ENSO seriously. Our research revealed that monthly CO_2 growth rate has a moderate, positive correlation relationship with MEI. We used geostatistics to predict and simulate the spatial distribution of CO_2 and found that in south of 12˚S, CO_2 concentration of ENSO warm episode is lower than the one of ENSO cold and neutral episodes. ENSO impacts CO_2 spatial distribution mainly in November, December, January and February; moderate-high concentration zone of ENSO warm episode more concentrates in the northern part of South America.

Keywords

CO_2 Growth Rate, ENSO, GOSAT TANSO, South America, Spatial Distribution of CO_2

1. Introduction

Climate change is one of the great challenges of the 21st century [1], Carbon dioxide (CO_2) is the most important

*Corresponding author.

How to cite this paper: Sun, Z.Y., Wang, X.F., Tani, H., Zhong, G.S. and Yin, S. (2016) Spatial Distribution of CO_2 Concentration over South America during ENSO Episodes by Using GOSAT Data. *American Journal of Climate Change*, **5**, 77-87.
http://dx.doi.org/10.4236/ajcc.2016.51009

greenhouse gas (GHG) in the atmosphere and is the greatest contributor to global warming [2]. The distribution of CO_2 is closely related to human survival, and international concerns about CO_2 are also getting stronger.

The impacts of CO_2-induced global warming include: Accelerating Sea Level Rise [3], Longer and More Damaging Wildfire Seasons [4], More Frequent and Intense Heat Waves [5], Costly and Growing Health Impacts [6], Heavier Precipitation and Flooding [7] and so on. Global temperatures in 2015 were the warmest on record, according to data published by meteorologists in the UK and US [8]. According to the Earth's CO_2 Home, the average global carbon dioxide (CO_2) concentration in December 2015 was 401.85 ppm, which is 3 ppm greater than in December 2014 [9]. 2015 not only was the warmest year on record, but also broke the record by the largest margin by which the record has been broken [8]. ENSO is one of the most important and longest-studied climate phenomena on the planet [10], and the strongest quasi-oscillatory pattern observed in the climate system; it is coupled to numerous climatic systems [11]. ENSO can affect global average temperatures; for example, in 1998 temperatures were significantly enhanced by strong El Niño conditions. 1998 remained the warmest year until 2005 and 2010 and the temperature of both of these years was enhanced by El Niño periods. The large margin by which 2015 is the warmest year is also attributed to another strong El Niño. However, 2014 was ENSO neutral (from the Multivariate ENSO Index (MEI): http://www.esrl.noaa.gov/psd/enso/mei/ and the Oceanic Nino Index (ONI): http://www.cpc.ncep.noaa.gov/products/analysis_monitoring/ensostuff/ensoyears.shtml). The only El Niño events in NOAA's 1950-2015 database comparable in strength to the one now developing occurred in 1982-1983 and 1997-1998 from the records ONI and MEI.

There are many complex relationships between carbon dioxide and ENSO from the viewpoints of climatology, geography, oceanography, ecology, biology and so on. From a simple viewpoint: marine dissolves a large number of CO_2 [12]; the increase in atmospheric CO_2 concentrations due to anthropogenic emissions has resulted in the oceans taking up CO_2 at a rate of about 7 $GtCO_2\ yr^{-1}$ [13] (the report published in 2005). As water temperature increases, its ability dissolving CO_2 decreases [14]. And the most obvious feature of the El Niño phenomenon is a wide range of abnormal warm seawater in central and eastern equatorial Pacific. Due to the response of the tropical ecosystem to climate variation, during ENSO warm phase, heterotrophic respiration will increase because in the water-stressed region photosynthesis it will be less, vice versa [15]. Therefore, there should be a relationship between CO_2 and ENSO. About the relationship between CO_2 and ENSO, many researchers have done a large number of studies mainly in two aspects: one is utilizing the climate model to predict or simulate the frequency and intensity of ENSO [16]-[19]; the ENSO response to global warming differs strongly from model to model and is thus highly uncertain. Some models simulate an increase in ENSO amplitude, others a decrease, and others virtually no change [20]. The other is utilizing historical observations to calculate or summarize the relationship and laws [11] [21]; some scholars use different algorithms to calculate the correlation relationship between CO_2 growth rate of lag times of 3, 6, 9, 12 months and ENSO Index [11] [22]. Patra, P. K. *et al*. estimate fluxes from 64 partitions of the globe using atmospheric CO_2 data from 87 stations worldwide by using time-dependent inverse (TDI) model [23] to analyze the relationship between CO_2 growth rates and ENSO episodes [24], and show that atmospheric CO_2 concentration and ENSO are positive correlation.

According to the summary of previous research, it is easy to find out that there is few research on the relationship between ENSO and distribution of CO_2, concentrating on using sampling observation data or station observation data. Since it is difficult to observe the global variation of GHG because the direct sampling of gases, especially in the upper atmosphere, requires great effort and cost [25]. Launching satellites to collect GHG data can solve this issue quite well. At present, the Thermal And Near infrared Sensor for carbon Observation (TANSO) aboard the Greenhouse gases Observing SATellite (GOSAT), launched in 2009 by Japan, is the first instrument dedicated to record CO_2 and methane (CH_4) concentrations (denoted XCO_2 and XCH_4, in ppm. XCO_2 and XCH_4 are column-averaged dry air mole fractions of atmospheric CO_2 and CH_4) [26] [27]. GOSAT make it possible to research the spatial distribution of CO_2, and know the impact of ENSO on CO_2 distribution. Although the SCanning Imaging Absorption spectroMeter for Atmospheric CHartographY (SCIAMACHY) aboard the ENVIronmentalSATellite (ENVISAT), launched in 2002 and lost in 2012 by the European Space Agency (ESA), can also retrieve GHG concentrations, but it is not specially designed for GHG retrieval and is not highly accurate; the single-measurement precision is approximately 1% - 2%, with an intermonth scatter of 2.3% [28] [29]. Therefore, before 2002, the CO_2 concentrations could not be measured directly using the remote sensing technique, maybe this is one reason why there is few study on the impact of ENSO on CO_2 spatial distribution.

El Niño, Warm phase of ENSO is one of three biggest natural disasters in South America, arid area will become wet, even occur the waterlogging in west coast, and oppositely large-scale droughts will happen in humid areas. In tropical South America, CO_2 flux anomaly is related to two basic meteorological parameters (rainfall and air temperature at 2 m) [24]. The concentration and spatial distribution of CO_2 will bring a huge impact on natural environment, such as rainforest, increasing CO_2 will lead to degradation of the Amazon rainforest [30] [31], and influence human life in South America. Facing one of the most severe El Niño, from Mar. 2015 to 2016, spatial distribution and changes of CO_2 will be much different from normal climate. In the present study, we analyzed CO_2 distribution by using GOSAT products from July 2009 to April 2014, got the relationship between CO_2 concentration and ENSO intensity by using the MEI and CO_2 data, from March 1958 to June 2015, from NOAA Earth System Research Laboratory. The objectives were: 1) to determine whether there is a relationship between CO_2 concentration and ENSO, 2) to examine the changes of CO_2 concentration distribution in South America during different phase of ENSO. This study explored the spatial distribution of CO_2 concentration of different ENSO episodes and also predicted the uncertainty distribution of CO_2 concentration in this El Niño which started in 2015, by using the distribution changes of CO_2 concentration in recent event, and explored the CO_2 concentration and distribution change during ENSO episode at a large spatial scale.

2. Materials and Methods

2.1. Study Area

The study region covers the majority of South America (12.4˚N - 53.9˚S, 34.8˚W - 81.3˚W, an area of 179.7 × 105 km^2) and includes Brazil, Argentina, Chile, Colombia and Bolivia, covering a total of 14 counties (**Figure 1**).

Figure 1. Land covers map (GlobCover image from 2011 downloaded from the homepage of the NEO: http://neo.sci.gsfc.nasa.gov/) in the study area.

In South America, the forest area is 920 million hectares, constituting 50% of the continent's area, constituting 23% of the world's forests [32]. Grassland area is approximately to 440 million hectares, constituting 25% of the continent's area, constituting more than 14% of the world's grasslands [32]. Agriculture is very important for South America's economy, since most countries in South America engaged in agricultural production, economic crops absolute dominance.

During ENSO warm phase, rainfall across the east-central and eastern Pacific Ocean, including several portions of the South American west coast, will increase due to El Niño's warm pool feeds thunderstorms above. If an ENSO warm episode occurred, weather it was strong or not, along the coasts of northern Peru and Ecuador, major flooding would be caused by warm and very wet weather from April to October. In opposite, During ENSO cold phase, the coastal regions of Peru and Chile will be very dry, but in the central Andes will be richer rainfall than normal even lead to catastrophic flooding, northern Brazil also will be wetter from December to February. South America is the continent which influenced by ENSO most directly and seriously.

2.2. Data

2.2.1. CO_2 Concentration Data

1) NOAA ESRL Data

Monthly mean atmospheric carbon dioxide at Mauna Loa Observatory, Hawaii measured as the mole fraction in dry air, on Mauna Loa (lat. 19.54˚N; long. 155.58˚W; height, 3397 m; interval, 1958-2016) constitute the longest record of direct measurements of CO_2 in the atmosphere. They were started by C. David Keeling of the Scripps Institution of Oceanography in March of 1958 at a facility of the National Oceanic and Atmospheric Administration [33]. Data are reported as a dry mole fraction defined as the number of molecules of carbon dioxide divided by the number of molecules of dry air multiplied by one million (ppm). Carbon dioxide measured at Mauna Loa Observatory was used to explore the relationship between CO_2 concentration and ENSO episode for a long duration. In the present study, we select the longest length of monthly data, from March 1958 to December 2015, to calculate the CO_2 monthly increasing rate, and to find out the relationship with ENSO.

2) GOSAT L3 Global CO_2 Distribution Data

The primary purpose of the GOSAT project is to accurately estimate the emissions and molecules of CO_2 in the atmosphere absorb light at particular wavelengths. The GOSAT uses the principle, the quantities of CO_2 in an optical path can be calculated by measuring the amount of light that is absorbed by molecules, to measure the concentrations of GHG in the atmosphere. GOSAT flies at an altitude of approximately 666 km and completes one revolution in about 100 minutes. The satellite returns to the same point in space in three days. Level 3 data products that are generated from Short Wavelength Infra-Red (SWIR) data observed by Thermal and Near-infrared Sensor for carbon Observation-Fourier Transform Spectrometer (TANSO-FTS) onboard GOSAT with the spatial resolution of 2.5˚ latitude × 2.5˚ longitude. L3 data generated by interpolating and extrapolating the FTS L2 data and estimating the distribution of XCO_2 for each month on a global scale. FTS SWIR L2 CO_2 column abundance products (denoted XCO_2, in ppm) contain column-averaged mixed volume ratios of CO_2 [34]. The XCO_2 represents the ratio of the total number of CO_2 molecules against that of dry air molecules, not only in the neighborhood of the Earth's surface but in the total vertical column extending to the top of the atmosphere [29]. The detailed algorithms and information for the TANSO-obtained GHG concentrations can be found from Greenhouse gases observing satellite GOSAT Official website
(https://data.gosat.nies.go.jp/GosatUserInterfaceGateway/guig/GuigPage/openTechInfo.do)

The GOSAT L3 global CO_2 distribution data were used in the present study to explore the spatial distribution changes of CO_2 of different ENSO episodes. The GOSAT L3 global CO_2 distribution has been published from June 2009 to July 2015, due to product version change, June 2014, December 2014, January 2015, February 2015 have not been published. Therefore, the CO_2 spatial distribution data during July 2009 to April 2010 (ENSO warm episode), July 2010 to April 2011 (ENSO cold episode), July 2011 to April 2012 (ENSO cold episode), July 2012 to April 2013 (ENSO neutral episode), July 2013 to April 2014 (ENSO neutral episode) were selected to analysis the spatial distribution of CO_2 under different ENSO events.

2.2.2. Multivariate ENSO Index (MEI) Data

Bimonthly MEI values (in 1/1000 of standard deviations), starting with December 1949/January 1950. ENSO is the most important coupled ocean-atmosphere phenomenon to cause global climate variability on interannual time scales [35]. People attempt to monitor ENSO by basing the Multivariate ENSO Index (MEI) on the six main observed variables over the tropical Pacific. MEI is a multivariate measure of the ENSO signal. These six variables are: sea-level pressure (P), zonal (U) and meridional (V) components of the surface wind, sea surface temperature (S), surface air temperature (A), and total cloudiness fraction of the sky (C) [36]. The MEI is computed separately for each of twelve sliding bi-monthly seasons (December/January, January/February, …, November/December). In order to keep the MEI comparable, all seasonal values are standardized with respect to each season and to the 1950-1993 reference period.

2.3. Method

Centralizing Second Moving Average Method

Second moving average method is calculating the second moving average of the first moving average, and then using the first moving average and second moving average to establish the trend model. The average values calculated by one moving average method have the shortcomings of lag bias. Especially, when the time-series data showing in a linear trend, moving average values always lag the observed data. Second moving average method can correct this lag bias, establishment the linear mathematical relationship with time to get the trend values. Second moving average method is applicable to the time-series analysis of the phenomenon which has clear trend change, also retains the advantages of first moving average method.

Centralizing refers calculating the average value of average 1 and average 2. Average 1 is the average from $t - n$ to t, average 2 is the average from t to $t + n$. n is half of one cycle length of the time-series data. This average is the trend value at time t. Trend value at time t, $f(t)$ can be expressed as follows:

$$f(t) = \frac{1}{2}\left(\frac{\sum_{i=t-n}^{i=t} D_i}{n} + \frac{\sum_{i=t}^{i=t+n} D_i}{n}\right) \tag{1}$$

where, n refers to one cycle length of time-series, monthly time data n is 6 months. D_i means observation data at time i. The length of trend time-series will be shorten, the beginning and ending n months cannot be calculated. This method is packaged as R's function (decompose()). Decompose a time series into seasonal, trend and irregular components using moving averages [37]. We got the trend data from monthly CO_2 concentration data by using function decompose() in R.

2.4. Data Processes

Logical process of this study is shown in **Figure 2**. Monthly CO_2 concentration data from March 1958 to December 2015, in total 694 months, were processed by using software R to remove the seasonal and random characteristics of the data, in this way trend CO_2 data can be extracted. According to R Software, time trend is decomposed by using centralizing second moving average method. Then using monthly trend CO_2 concentration data to calculate the monthly change rate of CO_2. Do correlation analysis of MEI and CO_2 change rates, if uncorrelated, that means there is no relationship between ENSO and CO_2 concentration increasing rate; if correlation, do the analysis on CO_2 spatial pattern during different ENSO phases. Using GOSAT L3 data to obtain monthly CO_2 concentration data over South America. Kriging interpolation method was utilized to predict the spatial unknown values, since GOSAT does not capture the column value when clouds are present [38]. Analysis the spatial correlation of CO_2 concentration respectively, in same month during ENSO neutral phase, warm phase and cold phase. If the space consistency is high, ENSO has no effects on the spatial distribution of the CO_2. Else, spatial relative difference would be analyzed to get the differences of CO_2 Spatial Patterns during different ENSO phase.

3. Results and Discussion

3.1. The Relationship between CO_2 Concentration and MEI

CO_2 trend calculated by utilizing centralizing second moving average method is shown in **Figure 3**. The data without seasonal and random characteristic has an obvious increasing trend. And the increasing rate is not always balancing on one level, higher in some months, lower in other months, but maintained an increasing trend.

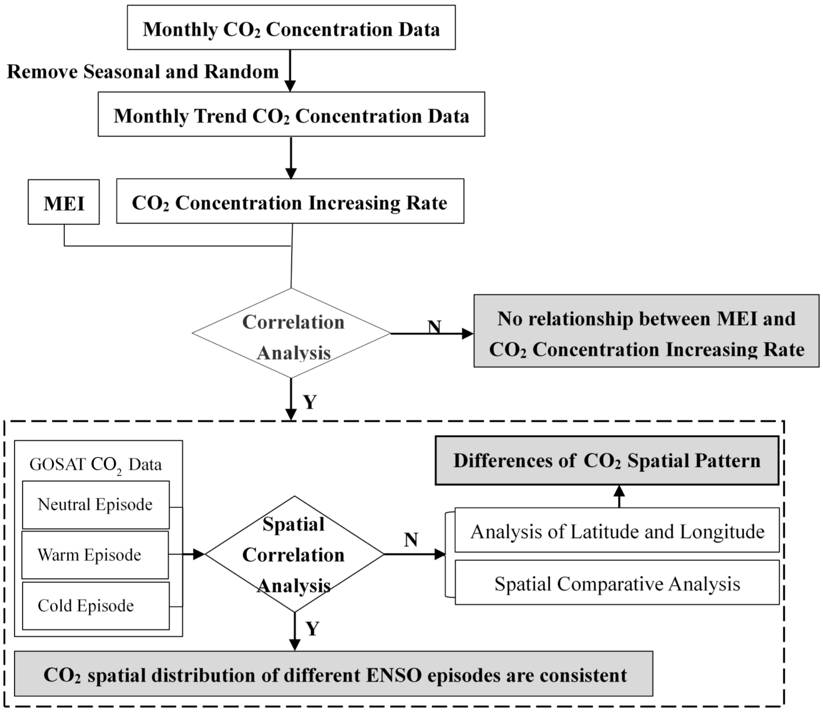

Figure 2. Logical flow of study.

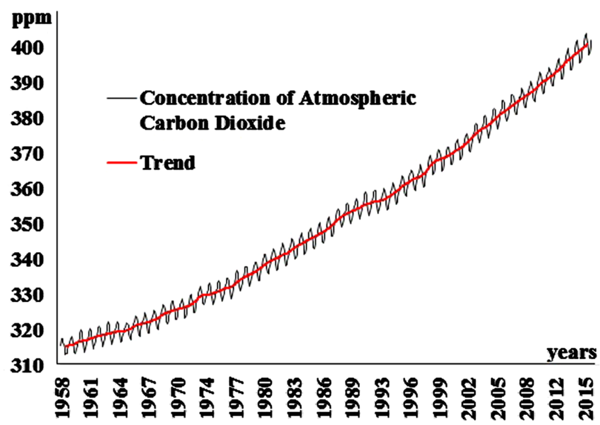

Figure 3. Time plot of monthly CO_2 concentration and trend.

In order to find out whether there is a relationship between CO_2 increasing rate and MEI, we get CO_2 increasing rate through derivation of trend values. Monthly CO_2 increasing rates and MEI values are shown in **Figure 4**.

From the whole view, two time series show the synchrony changes, except for from 1991 to 1993. Two time series were correlation analyzed by using EXCEL 2013, there is a significant correlation between both with the correlation coefficient 0.398, and $p = 0.000$. There is a moderate correlation relationship between CO_2 monthly increasing rate and MEI values from the viewpoint of statistics.

To explain the absence of synchrony around 1991, for a few years after a major volcanic eruption (*i.e.*, when there is an abundance of sulphate aerosols in the atmosphere), heterotrophic respiration decreases due to a lowering of the Earth's surface temperature and the productivity of forest ecosystems increases under enhanced diffuse radiation [22]. Both processes lead to a negative anomaly in CO_2 growth rate. In June 1991, in the same tropical latitude and upwind of Mauna Loa, there is a violent eruption of Mount Pinatubo, the second largest eruption of the twentieth century. That may the main reason of the absence of synchrony from 1991 to 1993 [11]. Remove the data from June 1991 to June 1993, the correlation coefficient between CO_2 monthly increasing rate

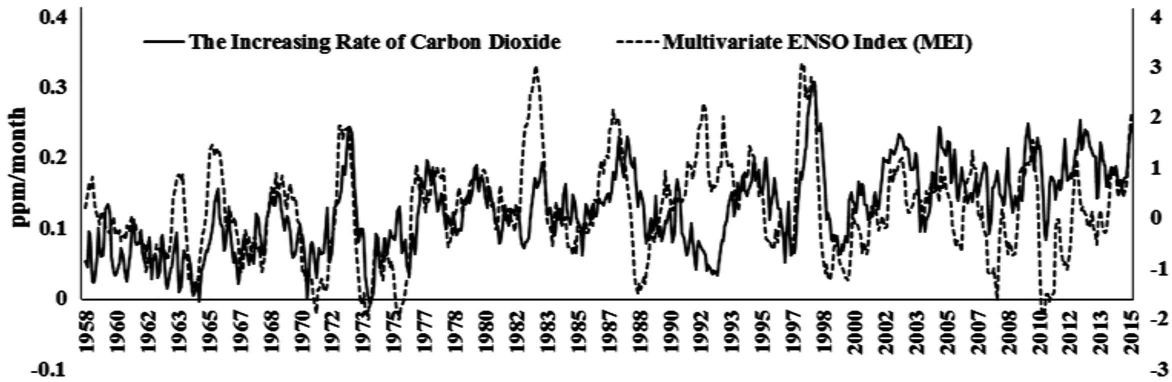

Figure 4. Time plot of monthly CO_2 concentration and trend.

and MEI values is 0.472, p = 0.000.

In summary, when MEI is high (ENSO warm episodes), CO_2 increasing rate reaches a peak with the exception of the interval around 1991, when MEI is low, ENSO cold episodes are followed by lower values of CO_2 increasing rate. ENSO and the increasing rate of CO_2 concentration show a positive correlation.

3.2. The Effects of ENSO on CO_2 Spatial Distribution

CO_2 concentration is increasing every year, in order to analysis the spatial distribution of different periods, the CO_2 concentration data need to be normalized to do comparative analysis. North-south span of South America is nearly 70 degrees, latitudinal variation of CO_2 spatial distribution is an obvious characteristic. Normalized values make it feasible to calculate different periods' spatial distribution characteristics, since the normalized values mean the relative amount in the spatial at one period. Latitudinal variation averages of normalized CO_2 spatial distribution during ENSO warm (one episode), cold (two episodes), and neutral (two episodes) phase were calculated by using ARCGIS 10.2 in the present study. The latitudinal spatial distributions of CO_2 concentration of each ENSO episode were shown in **Figure 5**.

July 2009 to April 2010 is ENSO warm episode, July 2010 to April 2011 and July 2011 to April 2012 are ENSO cold episodes, July 2012 to April 2013 and July 2013 to April 2014 are ENSO neutral episodes, according to the MEI shown in **Table 1**. CO_2 concentration curves of ENSO neutral and cold episodes have the consistent trend and two peaks, respectively around 3˚S and 20˚S. There is no apparent inconsistencies feature between ENSO cold episode and ENSO neutral episode. But the peak of ENSO warm episode curve (red point line in **Figure 5**) approximately to 7˚S, with no two peaks, and high value range, from 3˚S to 20˚S, is very stable. South of 12˚S, the value of ENSO warm episode is lower than ones of ENSO cold and neutral episodes. That means, during ENSO warm phase, south of 12˚S in South America, CO_2 concentration is relatively low, more concentrated in Northern South America, relative northward.

Overall, CO_2 spatial distribution of ENSO warm episode is different from ENSO cold and neutral episodes, but more detailed spatial and temporal characteristics are needed for further study. Monthly CO_2 spatial data during different ENSO phase were analyzed by using spatial correlation analysis. This method can help us to know the differences in places and periods. The results of spatial correlation analysis with ENSO warm episode are shown in **Table 1**.

From the results of spatial correlation analysis, it is easily to find out that spatial distributions of CO_2 during ENSO warm phase and ENSO cold phase are highly correlated to each other except for November, December, January, February and March, spatial pattern are basically the same in geostatistics. From November to March, CO_2 spatial pattern between ENSO warm episode and ENSO cold episode are not highly synchrony. For ENSO neutral episode, high absence of synchrony is from November to February. We can also know that there is no relationship between spatial correlation coefficient and MEI values, from the box in **Table 1**. In northern hemisphere winter, the CO_2 spatial distribution of different ENSO episodes is most different.

For figuring out the detailed differences of CO_2 spatial pattern among ENSO warm, cold, neutral episodes, the average CO_2 spatial distribution normalized data of November, December, January and February in different ENSO episodes are shown in **Figure 6**.

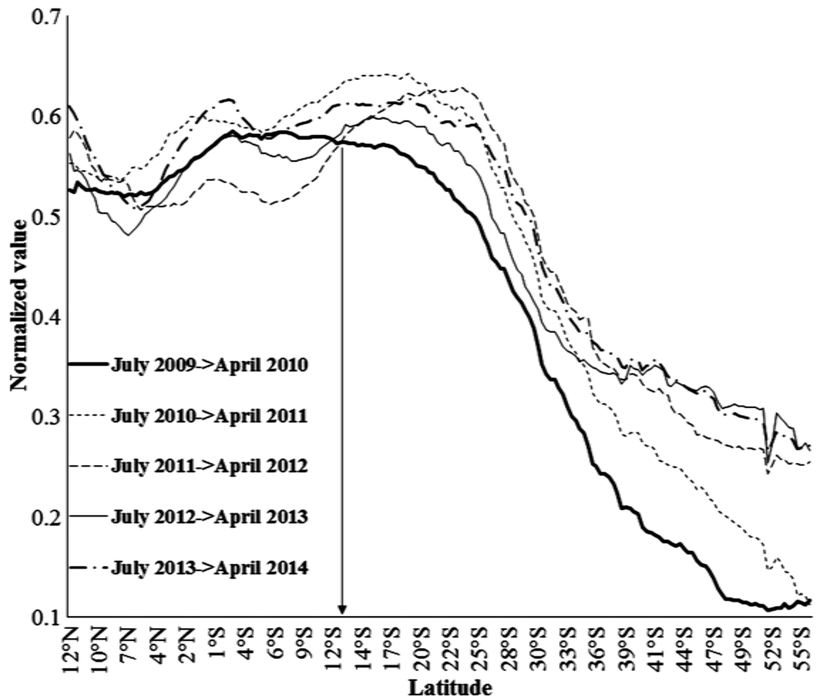

Figure 5. The latitudinal spatial distributions of CO_2 concentration of each ENSO episode normalized value.

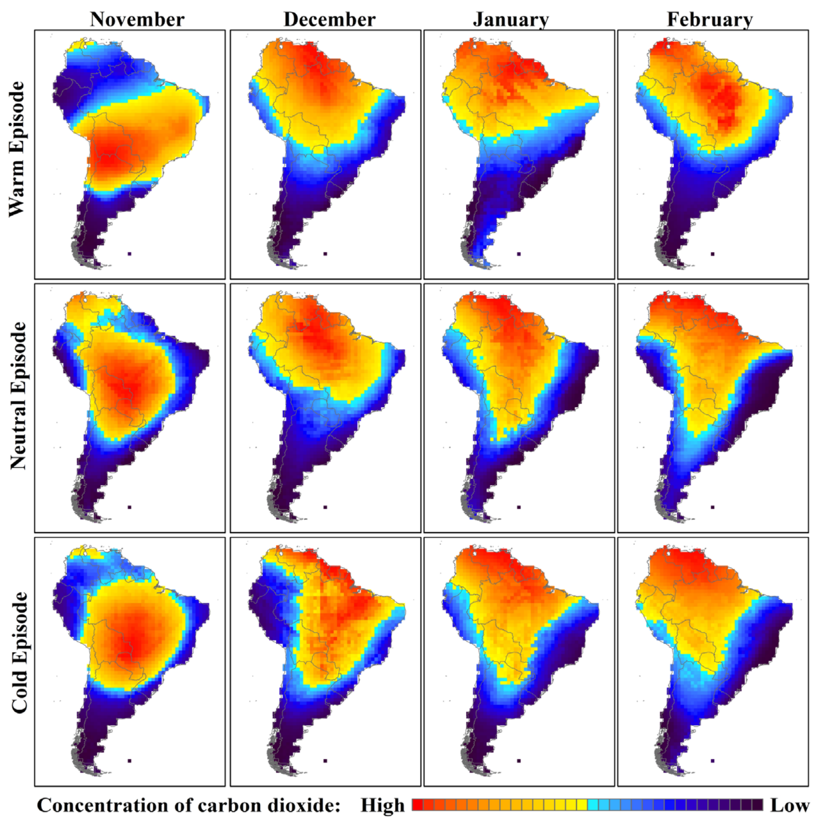

Figure 6. Spatial distribution of CO_2 concentration from November to February of different ENSO episodes.

Table 1. MEI values and spatial correlation coefficient of spatial distribution of CO_2 during ENSO warm, neutral and cold phase.

ENSO Warm Episode		ENSO Cold Episode		ENSO Cold Episode		ENSO Neutral Episode		ENSO Neutral Episode	
2009	2010	2010	2011	2011	2012	2012	2013	2013	2014
Month	MEI	R	MEI	R	MEI	R	MEI	R	MEI
Jul.	1.00	0.89	−1.07	0.93	−0.05	0.88	1.17	0.87	−0.37
Aug.	0.99	0.72	−1.78	0.87	−0.44	0.9	0.58	0.89	−0.53
Sep.	0.81	0.86	−1.95	0.88	−0.71	0.92	0.33	0.89	−0.10
Oct.	1.04	0.8	−1.9	0.83	−0.94	0.86	0.14	0.85	0.14
Nov.	1.09	0.64	−1.52	0.69	−0.89	0.65	0.21	0.31	−0.03
Dec.	1.04	0.19	−1.53	0.52	−0.91	0.78	0.08	0.6	−0.26
Jan.	1.15	0.49	−1.68	0.26	−1.05	0.21	0.04	0.86	−0.31
Feb.	1.52	0.78	−1.56	0.57	−0.71	0.7	0.04	0.4	−0.26
Mar.	1.39	0.46	−1.56	0.56	−0.43	0.84	0.04	0.72	0.01
Apr.	0.89	0.81	−1.48	0.84	0.05	0.68	0.04	0.86	0.19

Moderate-high CO_2 concentration were expressed as warm color, in opposite, Moderate-low ones were expressed as cold color, and images were stretched by using histogram equalize to enhance the contradistinction. During ENSO warm phase: in November, moderate-high CO_2 concentration concentrate in central part of South American continent, from about 5˚S to 30˚S; in December, moderate-high CO_2 concentration zone move northward, concentrate in northern part; moderate-high CO_2 concentration zone in January and February are almost the same to the one in December. During ENSO neutral phase: moderate-high CO_2 concentration concentrate in central part of South American continent same with ENSO cold episode, and further north than ENSO warm episode; in December, synchronized with ENSO warm episode, moderate-high CO_2 concentration zone move northward; in January, moderate-high CO_2 concentration zone extend to southward, and the distribution in February is almost the same to January. During ENSO cold phase: in November, the pattern is consistent with ENSO neutral episode; from November to December, moderate-high CO_2 concentration zone extend to northward; the spatial distribution in December, January and February are substantially the same pattern. In summary, the distribution in November of ENSO cold episode and ENSO neutral episode are consistent, moderate-high CO_2 concentration located in further north than that during ENSO warm phase; in December, the distribution during ENSO cold phase are consistent with that during ENSO neutral phase, moderate-high CO_2 concentration concentrated in northern part; in January and February, moderate-high CO_2 concentration zone of ENSO cold and neutral episode extend to more south than ENSO warm episode. CO_2 concentration during ENSO warm phase is more nonuniform than the ones during ENSO cold and neutral phase, concentrate in northern part of South American continent.

4. Conclusion

In this study, South America as one of zones most influenced by ENSO event was selected as the study area. Long duration CO_2 concentration sample data and monthly spatial remote sensing CO_2 concentration data were used to analyze the effects of ENSO on CO_2 concentration, including increasing concentrations and spatial distribution. Trend CO_2 data were calculated from monthly data by using removal seasonal and random method, centralizing second moving average method, in software R. There is a moderate correlation between monthly increasing rate of CO_2 concentration and MEI. ENSO events have an effect on increasing rate of CO_2 concentration. Comparing the impact of ENSO on CO_2 spatial distribution in south of 12˚S of South America, concentration of ENSO warm episode is obviously lower than concentration of ENSO cold and neutral episodes. Through spatial correlation analysis, the months seriously influenced by ENSO condition can be found out. They are November, December, January, February, when northern hemisphere is winter and ENSO episode peaks [39].

Moderate-high CO_2 concentration of ENSO warm episode is located in more north and nonuniform than that of ENSO cold and neutral episode. The spatial distribution in South America and increasing rate of CO_2 concentration are affected by ENSO significantly. The results of the present study also provide supports to predict the effects of the super ENSO warm episode which started from 2015.

Acknowledgements

This study was carried out under the Joint Research Program of Arid Land Research Center, Tottori University. MEI and CO_2 data are obtained from NOAA Earth System Research Laboratory. We also thank the GOSAT project of Japan for providing data used in this study. ARCGIS 10.2 and R are used in computational processing of this research.

References

[1] Mitigation, C.C. (2011) IPCC Special Report on Renewable Energy Sources and Climate Change Mitigation.

[2] Davidson, O., Bosch, P., Dave, R. and Meyer, L. (2007) Mitigation of Climate Change. Cambridge University Press, Cambridge.

[3] Nicholls, R.J. and Cazenave, A. (2010) Sea-Level Rise and Its Impact on Coastal Zones. *Science*, **328**, 1517-1520. http://dx.doi.org/10.1126/science.1185782

[4] Liu, Y., Stanturf, J. and Goodrick, S. (2010) Trends in Global Wildfire Potential in a Changing Climate. *Forest Ecology and Management*, **259**, 685-697. http://dx.doi.org/10.1016/j.foreco.2009.09.002

[5] Meehl, G.A. and Tebaldi, C. (2004) More Intense, More Frequent, and Longer Lasting Heat Waves in the 21st Century. *Science*, **305**, 994-997. http://dx.doi.org/10.1126/science.1098704

[6] Hill, J., Polasky, S., Nelson, E., Tilman, D., Huo, H., Ludwig, L., Ludwig, L., Neumann, J., Zheng, H. and Bonta, D. (2009) Climate Change and Health Costs of Air Emissions from Biofuels and Gasoline. *Proceedings of the National Academy of Sciences*, **106**, 2077-2082. http://dx.doi.org/10.1073/pnas.0812835106

[7] Trenberth, K.E. (2011) Changes in Precipitation with Climate Change. *Climate Research*, **47**, 123. http://dx.doi.org/10.3354/cr00953

[8] McGrath, M. (2016) Climate Change: 2015 ‘Shattered’ Global Temperature Record by Wide Margin. BBC Science and Environment News. http://www.bbc.com/news/science-environment-35354579

[9] Earth’s CO_2 (2016) https://www.CO_2.earth/

[10] Lovejoy, T.E. (2006) Climate Change and Biodiversity. The Energy and Resources Institute (TERI).

[11] Mazzarella, A., Giuliacci, A. and Scafetta, N. (2013) Quantifying the Multivariate ENSO Index (MEI) Coupling to CO_2 Concentration and to the Length of Day Variations. *Theoretical and Applied Climatology*, **111**, 601-607. http://dx.doi.org/10.1007/s00704-012-0696-9

[12] Feely, R.A., Sabine, C.L., Lee, K., Berelson, W., Kleypas, J., Fabry, V.J. and Millero, F.J. (2004) Impact of Anthropogenic CO_2 on the $CaCO_3$ System in the Oceans. *Science*, **305**, 362-366. http://dx.doi.org/10.1126/science.1097329

[13] Metz, B., Ed. (2005) Carbon Dioxide Capture and Storage: Special Report of the Intergovernmental Panel on Climate Change. Cambridge University Press, Cambridge.

[14] Riebeek, H. (2008) The Ocean’s Carbon Balance. NASA Earth Observatory Feature Article. http://earthobservatory.nasa.gov/Features/OceanCarbon/printall.php

[15] Patra, P.K., Maksyutov, S., Ishizawa, M., Nakazawa, T., Takahashi, T. and Ukita, J. (2005) Interannual and Decadal Changes in the Sea-Air CO_2 Flux from Atmospheric CO_2 Inverse Modeling. *Global Biogeochemical Cycles*, **19**.

[16] Timmermann, A., Oberhuber, J., Bacher, A., Esch, M., Latif, M. and Roeckner, E. (1999) Increased El Niño Frequency in a Climate Model Forced by Future Greenhouse Warming. *Nature*, **398**, 694-697. http://dx.doi.org/10.1038/19505

[17] Knutson, T.R., Manabe, S. and Gu, D. (1997) Simulated ENSO in a Global Coupled Ocean-Atmosphere Model: Multidecadal Amplitude Modulation and CO_2 Sensitivity. *Journal of Climate*, **10**, 138-161. http://dx.doi.org/10.1175/1520-0442(1997)010<0138:SEIAGC>2.0.CO;2

[18] Knutson, T.R. and Manabe, S. (1994) Impact of Increased CO~ 2 on Simulated ENSO-Like Phenomena. *Geophysical Research Letters*, **21**, 2295-2298. http://dx.doi.org/10.1029/94GL02152

[19] Merryfield, W.J. (2006) Changes to ENSO under CO_2 Doubling in a Multimodel Ensemble. *Journal of Climate*, **19**, 4009-4027. http://dx.doi.org/10.1175/JCLI3834.1

[20] Latif, M. and Keenlyside, N.S. (2009) El Niño/Southern Oscillation Response to Global Warming. *Proceedings of the National Academy of Sciences*, **106**, 20578-20583. http://dx.doi.org/10.1073/pnas.0710860105

[21] Malone, S.L., Staudhammer, C.L., Oberbauer, S.F., Olivas, P., Ryan, M.G., Schedlbauer, J.L., Loescher, H.W. and Starr, G. (2014) El Niño Southern Oscillation (ENSO) Enhances CO_2 Exchange Rates in Freshwater Marsh Ecosystems in the Florida Everglades. *PLoS ONE*, **9**, e115058. http://dx.doi.org/10.1371/journal.pone.0115058

[22] Patra, P.K., Maksyutov, S. and Nakazawa, T. (2005) Analysis of Atmospheric CO_2 Growth Rates at Mauna Loa Using CO_2 Fluxes Derived from an Inverse Model. *Tellus B*, **57**, 357-365. http://dx.doi.org/10.1111/j.1600-0889.2005.00159.x

[23] Gurney, K.R., Law, R.M., Denning, A.S., Rayner, P.J., Pak, B.C., Baker, D., *et al*. (2004) Transcom 3 Inversion Intercomparison: Model Mean Results for the Estimation of Seasonal Carbon Sources and Sinks. *Global Biogeochemical Cycles*, **18**, GB1010. http://dx.doi.org/10.1029/2003GB002111

[24] Patra, P.K., Ishizawa, M., Maksyutov, S., Nakazawa, T. and Inoue, G. (2005) Role of Biomass Burning and Climate Anomalies for Land-Atmosphere Carbon Fluxes Based on Inverse Modeling of Atmospheric CO_2. *Global Biogeochemical Cycles*, **19**, GB3005. http://dx.doi.org/10.1029/2004GB002258

[25] Ishida, H., Nakjima, T.Y., Yokota, T., Kikuchi, N. and Watanabe, H. (2011) Investigation of GOSAT TANSO-CAI Cloud Screening Ability through an Intersatellite Comparison. *Journal of Applied Meteorology and Climatology*, **50**, 1571-1586. http://dx.doi.org/10.1175/2011JAMC2672.1

[26] Oguma, H., Morino, I., Suto, H., Yoshida, Y., Eguchi, N., Kuze, A. and Yokota, T. (2011) First Observations of CO_2 Absorption Spectra Recorded in 2005 Using an Airship-Borne FTS (GOSAT TANSO-FTS BBM) in the SWIR Spectral Region. *International Journal of Remote Sensing*, **32**, 9033-9049. http://dx.doi.org/10.1080/01431161.2010.535864

[27] Reuter, M., Buchwitz, M., Schneising, O., Heymann, J., Bovensmann, H. and Burrows, J.P. (2010) A Method for Improved SCIAMACHY CO_2 Retrieval in the Presence of Optically Thin Clouds. *Atmospheric Measurement Techniques*, **3**, 209-232. http://dx.doi.org/10.5194/amt-3-209-2010

[28] Hill, M.J., Held, A.A., Leuning, R., Coops, N.C., Hughes, D. and Cleugh, H.A. (2006) MODIS Spectral Signals at a Flux Tower Site: Relationships with High-Resolution Data, and CO_2 Flux and Light Use Efficiency Measurements. *Remote Sensing of Environment*, **103**, 351-368. http://dx.doi.org/10.1016/j.rse.2005.06.015

[29] Guo, M., Wang, X., Li, J., Yi, K., Zhong, G. and Tani, H. (2012) Assessment of Global Carbon Dioxide Concentration Using MODIS and GOSAT Data. *Sensors*, **12**, 16368-16389. http://dx.doi.org/10.3390/s121216368

[30] Cox, P.M., Betts, R.A., Jones, C.D., Spall, S.A. and Totterdell, I.J. (2000) Acceleration of Global Warming Due to Carbon-Cycle Feedbacks in a Coupled Climate Model. *Nature*, **408**, 184-187. http://dx.doi.org/10.1038/35041539

[31] Radford, T. (2002) The Guardian: "World May Be Warming up Even Faster". http://www.theguardian.com/environment/2000/nov/09/weather.climatechange1

[32] Yang, H. (2013) The Analysis on the Possible Overseas Transfer Destination of Chinese Manufacturing Industry. *Journal of International Trade*, No. 4, 123-138.

[33] Keeling, C.D., Bacastow, R.B., Bainbridge, A.E., Ekdahl, C.A., Guenther, P.R., Waterman, L.S. and Chin, J.F. (1976) Atmospheric Carbon Dioxide Variations at Mauna Loa Observatory, Hawaii. *Tellus*, **28**, 538-551. http://dx.doi.org/10.1111/j.2153-3490.1976.tb00701.x

[34] Bril, A., Oshchepkov, S. and Yokota, T. (2012) Application of a Probability Density Function-Based Atmospheric Light-Scattering Correction to Carbon Dioxide Retrievals from GOSAT Over-Sea Observations. *Remote Sensing of Environment*, **117**, 301-306. http://dx.doi.org/10.1016/j.rse.2011.10.005

[35] Wolter, K. and Timlin, M.S. (1993) Monitoring ENSO in COADS with a Seasonally Adjusted Principal Component Index. *Proceedings of the* 17*th Climate Diagnostics Workshop*, Norman, 18-23 October 1992, 52-57.

[36] Wolter, K. and Timlin, M.S. (1998) Measuring the Strength of ENSO Events: How Does 1997/98 Rank? *Weather*, **53**, 315-324. http://dx.doi.org/10.1002/j.1477-8696.1998.tb06408.x

[37] Kendall, M. and Stuart, A. (1983) The Advanced Theory of Statistics. Vol. 3: Distribution Theory. Griffin, London, 410-414.

[38] Liu, Y., Wang, X., Guo, M. and Tani, H. (2012) Mapping the FTS SWIR L2 Product of XCO_2 and XCH_4 Data from the GOSAT by the Kriging Method—A Case Study in East Asia. *International Journal of Remote Sensing*, **33**, 3004-3025. http://dx.doi.org/10.1080/01431161.2011.624132

[39] Latif, M. and Grötzner, A. (2000) The Equatorial Atlantic Oscillation and Its Response to ENSO. *Climate Dynamics*, **16**, 213-218. http://dx.doi.org/10.1007/s003820050014